Proceedings

1995 IEEE/RSJ International Conference on Intelligent Robots and Systems

Human Robot Interaction and Cooperative Robots

August 5 – 9, 1995

Pittsburgh, Pennsylvania USA

Co-sponsored by

IEEE Industrial Electronics Society
IEEE Robotics and Automation Society
Robotics Society of Japan (RSJ)
Society of Instrument and Control Engineers (SICE)
New Technology Foundation

Volume 2

IEEE Computer Society Press
Los Alamitos, California

Washington • Brussels • Tokyo

A New Consideration on Active Antenna

Makoto Kaneko, Naoki Kanayama, and Toshio Tsuji

Industrial and Systems Engineering
Hiroshima University
Higashi-Hiroshima 724 JAPAN

Abstract

This paper discusses the sensing accuracy of the Active Antenna that can detect the contact location between an insensitive flexible beam and an environment through the measurement of the rotational compliance of the beam in contact with the environment. During pushing motion of antenna, the contact point generally shifts on the environment's surface, which either underestimates or overestimates the rotational compliance and eventually brings a sensing error for localizing the contact point. The goal of this paper is to consider the effect of the environment's curvature on the rotational compliance. We show that the rotational compliance of the antenna being in contact with a curved environment depends on not only the contact distance but also on a new non-dimensional parameter including the pushing angle and the environment's curvature where the antenna makes contact. We further show experimental results to support the theoretical analysis for various environments with different curvature.

Key words: Active sensing, Active Antenna, Tactile sensing, Contact point, Sensing accuracy, Environment's curvature

1. Introduction

Active Antenna is a sensing system enabling us to detect the contact location through the measurement of the rotational compliance of an insensitive antenna in contact with an environment. In our former work, we have shown that for a planar type Active Antenna, the contact location is a function of the rotational compliance alone, and that one active motion is necessary and sufficient for localizing the contact point irrespective to friction at the point of contact, if the straight beam is utilized [1], [2]. We have also shown the basic structure of 3D Active Antenna and its sensing algorithm [3]. A big advantage of Active Antenna is that a contact point is obtained through a surprisingly simple active motion, while sophisticated active motions should be prepared for most of contact sensing to avoid a large force between sensor and environment. This is because the flexibility of the antenna successfully relaxes the contact force by itself, even under a large positional error.

The Active Antenna is composed of an insensitive flexible beam, actuators to move the beam, position sensors to measure the actuator position, and one-axis (for 2D) or two-axis (for 3D) moment sensor. At the beginning of sensing, the antenna approaches an environment until it makes contact. Since this approach phase is exactly the same as the one discussed in other tactile based active sensing [4], we do not focus on the approach phase in this paper. Thus, we suppose that at the initial state, the antenna is already in contact with the environment. In the active motion, we simply push the antenna to the environment. During this, the rotational compliance in contact with the environment is computed based on both torque and position sensor outputs. In our former work [1], it is shown that the rotational compliance in contact with the environment is proportional to the contact length, which is the basic principle of the Active Antenna. In the explanation of the basic principle, we implicitly assume that the antenna makes contact with a sharp edged object, and, therefore, the contact point does not change over the environment, while a longitudinal slip inevitably occurs to satisfy the geometrical relationship between the antenna shapes before and after a bending deformation which brings the movement of the contact point along the longitudinal direction over the antenna. If the environment has a finite curvature, however, the contact point moves continuously on the environment during the pushing motion. As a result, the contact point will shift close to the joint of the antenna. Since the equivalent contact distance becomes shorter after the active motion, the rotational compliance should be a bit smaller than that of the antenna being in contact with a sharp edged object. Unfortunately, in most case, we do not have any preliminary information about the environment's geometry. It is, therefore, important for us to evaluate how much the sensing accuracy is deteriorated by the environment's geometry.

After briefly reviewing conventional works dealing with environment perception using a flexible beam, we first discuss the effect of the environment's geometry on the sensing accuracy, and introduce a new non dimensional parameter h which controls the rotational compliance during

0-8186-7108-4/95 $4.00 © 1995 IEEE

the pushing motion. The parameter is composed of the radius of curvature at the point of contact, the pushing angle, and the contact distance itself. We show that the contact distance is no longer the function of the rotational compliance C_θ alone when the antenna makes contact with the environment whose curvature is finite, and varies according to the non dimensional parameter h as well as the contact distance s_x, namely, $C_\theta = f(h, s_x)$. Through the simulation analysis, we show that if the contact distance is less than the radius of curvature at the point of contact and the pushing angle is less than 5 degrees, the sensing error can be suppressed within 4 %. Thus, it is shown that the influence of the environment's curvature on the sensing error is negligibly small for most of environments. We also show that the experimental results reasonably support both simulation and analytical results.

II. Related Works

A simple flexible beam sensor can take the form of a short length of spring piano wire or hypodermic tubing anchored at the end. When the free end touches an external object, the wire bends. This can be sensed by a piezoelectric element or by a simple switch [5]. A more elaborate sensor is described by Wang and Will [6]. Long antennae-like whisker sensors were mounted on the SRI mobile robot, Shakey [7], and on Rodney Brook's six-legged robot insects [8]. Hirose, et. al. discussed the utilization of whisker sensors in legged robots [9]. The sensor system is composed of an electrode and a whisker whose end is fixed at the base. This sensor unit has been arranged in an array around each foot of the legged robot, Titan III, so that it can monitor the separation between each foot and the ground to allow deceleration of the foot before contact. This sensor is also conveniently used to confirm which part of the foot is in contact with the ground. Similarly shaped whiskers have been considered for legs of the Ohio State University active suspension vehicle [10]. Russell has developed a sensor array [11] by mounting whisker sensors on a mobile robot, and succeeded in reconstructing the shape of a convex object followed by the whisker. In his work, it is assumed that the whisker tip is always in contact with the environment, and that when the whisker contacts the environment except for the tip, it is assigned to a failure mode. The major difference between previous works [5]-[11] and ours is that the Active Antenna enables us to localize a contact point between the beam and the environment, while previous works do not.

On the other hand, Tsujimura and Yabuta have addressed an object shape detection system using a force/torque sensor and an insensitive flexible probe [12]. This approach is based on the original idea that force/torque information makes it possible to estimate a contact location as well as a contact force, which was first pointed out by Salisbury [13]. Later, it was extended to more general and mathematical forms by Brock and Chiu [14], Tsujimura and Yabuta [15], and Bicchi [16]. These approaches [12]-[16] can be categorized into passive sensing without utilizing any active motion for localizing the contact point.

III. Basic Structure and Working Principle of Active Antenna

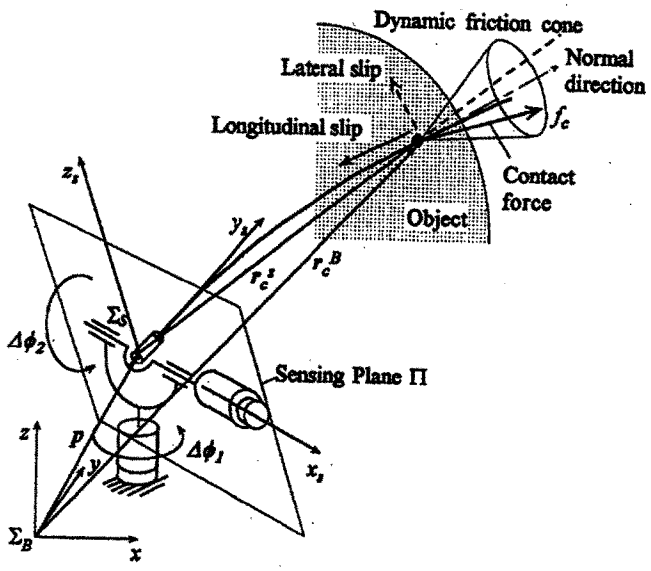

Fig.1 An example of 3D Active Antenna

Fig.1 shows an overview of the 3D Active Antenna and its coordinate system, where Σ_B (or upper script "B") and Σ_s (or upper script "s") denote the base coordinate system and the sensor coordinate system, respectively. The 3D Active Antenna is composed of an insensitive flexible beam, two actuators to move the beam in 3D space, two position sensors to measure the angular displacements θ and ϕ, and a two-axis moment sensor to detect moments around both x_s and z_s axes. The moment sensor is designed so that each sensing axis can intersect with the center of rotation (the origin of the sensor coordinate system). Now, let us define the sensing plane Π, with the plane spanned by two unit vectors whose directions coincide with x_s and y_s. The design orientation taken for the two-axis moment sensor enables us to evaluate the direction of the contact force projected on the plane Π from the outputs of the moment sensor. Although due to the lack of the information on the contact distance, the exact contact force can not be detected by the two-axis moment sensor, we can easily evaluate the direction of contact force on Π through the information of moment sensor. When we assume a beam whose compliance is uniform for every direction in the plane perpendicular to the longitudinal direction of the beam, the reaction force always appears the exactly opposite direction against the displacement of the beam. The major difference between 2D and 3D Active Antennae is that a lateral slip may possibly occur for a 3D version, while we never assume it for a 2D one. Thus, the main issue for 3D Active Antenna is how to detect an appearance of lateral slip, and how finally to detect

the contact distance under the situation given. In our former work[3], we have explored this matter and shown that two-axis moment sensor allows us to examine the appearance of a lateral slip by checking the angle between the pushing direction and contact force observed on Π. We have further shown an algorithm eventually detecting the normal direction on the surface of the environment. Once we detect the normal direction, the problem results in that of 2D Active Antenna, since the lateral slip can be blocked out perfectly under a pushing motion against the normal direction of the environment.

IV. Effect of the Environment's Geometry on Sensing Accuracy

4.1 Main assumptions

For simplifying our discussions, we set the following assumptions:

Assumption 1 : The antenna deformation is small enough to ensure that we can apply a linear approximation.

Assumption 2 : The compliance of the environment is sufficiently small compared with that of the antenna.

Assumption 3 : Before applying an active motion, the antenna is already in contact with an environment with zero force.

Assumption 4 : The base of antenna has one degree-of-freedom for rotation and the environment is 2D.

Since the problem, localizing contact point, results in that of 2D Active Antenna when the 3D Active Antenna detects the normal direction of environment's surface, the final sensing accuracy is same for both 2D and 3D versions. Therefore, to simplify the discussion, with assumption 4, we consider the effect of environment's geometry on sensing accuracy by utilizing a 2D model.

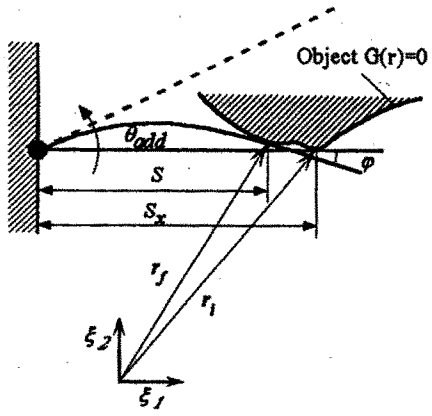

Fig.2 A 2D Active Antenna contacting an environment

4.2 Effect of the Environment's Geometry

Let us assume a 2D Active Antenna contacting an environment as shown in Fig.2, where θ_{add}, S_x, and S are the pushing angle, the initial contact length, and the final contact length, respectively, and the dotted line denotes the antenna's shape without the environment when θ_{add} is imparted. The lower subscripts "i" and "f" denote initial and final values, respectively. If the environment has a sharp edge at the initial contact point, S_x, and S should be exactly same each other. However, they are no longer same when it has an appropriate curvature at the point of contact with the antenna. We assume that the object shape is imparted by the function of G(r)=0, where r is a position vector whose origin is given at an arbitrary point as shown in Fig.2, and ξ_1 and ξ_2 are the unit vectors perpendicular each other. For our convenience, we choose the direction of ξ_1 is so determined that it coincides with the longitudinal direction of the initial beam posture.

First of all, let us qualitatively consider the effect of the shift of contact point during sensing. As seen from Fig.2, the shift of contact point can be decomposed into the $-\xi_1$ and ξ_2 directional shifts which bring two different effects for the rotational compliance around the base. The $-\xi_1$ directional shift contributes to reducing the rotational compliance, while the ξ_2 directional one to increasing it. Thus, these two shifts act on the rotational compliance so that they may cancel each other, though the degree of cancellation strongly depends on the environment's curvature at the point of contact, on the contact length, and on how much pushing angle is imparted.

Since the ξ_1 directional shift of the contact point is expressed by $-\xi_1^t(\mathbf{r}_f-\mathbf{r}_i)$, S_x-S is given by,

$$S_x - S = -\xi_1^t(\mathbf{r}_f-\mathbf{r}_i). \tag{1}$$

Similarly, the ξ_2 directional shift of the contact point is obtained by,

$$\frac{fS^3}{3EI} = S\theta_{add} - \xi_2^t(\mathbf{r}_f-\mathbf{r}_i) \tag{2}$$

where E, I, and f are modulus of elasticity of the beam, the second moment of the cross section of the antenna, and the ξ_2 directional contact force component, respectively. Since a normal direction on the environment's surface is represented by $\nabla G(\mathbf{r})$, φ defined in Fig.2 is given by,

$$\varphi \approx \tan\varphi = \frac{\|\nabla G(\mathbf{r}_f)\times\nabla G(\mathbf{r}_i)\|}{\nabla G(\mathbf{r}_f)\times\nabla G(\mathbf{r}_i)}. \tag{3}$$

Since the displacement angle of the antenna is equal to $\varphi+\theta_{add}$, the following relationship holds,

$$\frac{fS^2}{2EI} = \theta_{add} + \varphi. \tag{4}$$

The joint torque is expressed by

$$\tau = Sf. \tag{5}$$

The rotational compliance $C_{\theta c}$ around the base is given by,

$$C_{\theta c} = \frac{\theta_{add}}{\tau} \tag{6}$$

where the subscript "c" means a curved object. These equations (1), (2), (4), (5), and (6) are basic ones for solving the relationship between the contact distance S and the rotational compliance $C_{\theta c}$.

Since the local environment's shape at the point of contact can be regarded as a part of circular whose radius is R, we can use a full circular object instead of an environment without losing any generality. Thus, hereafter, we utilize a circular object with the following mathematical form.

$$G(r) = \|r\text{-}r_0\|\text{-}R = 0 \tag{7}$$

where r_0 is the position vector pointing the center of the circle. From eq.(7),

$$\nabla G(r) = \frac{r - r_0}{R}. \tag{8}$$

Therefore, we obtain

$$\|\nabla G(r)\| = \frac{\|r - r_0\|}{R} = 1. \tag{9}$$

By taking eq.(8) into consideration, $r_f - r_i$ is alternatively expressed by,

$$r_f - r_i = R\{\nabla G(r_f) - \nabla G(r_i)\} \tag{10}$$

Since

$$\xi_2 = -\frac{\nabla G(r_i)}{\|\nabla G(r_i)\|} = -\nabla G(r_i), \tag{11}$$

the ξ_2 directional shift of the contact point is given by,

$$\begin{aligned} &\xi_2^t(r_f - r_i) \\ &= -\{\nabla G(r_i)\}^t R\{\nabla G(r_f) - \nabla G(r_i)\} \\ &= -R\|\nabla G(r_f)\| \|\nabla G(r_i)\|\cos\varphi + R\|\nabla G(r_i)\|^2 \\ &= R(1\text{–}\cos\varphi). \end{aligned} \tag{12}$$

On the other hand, taking the relationship $\xi_2 = -\nabla G(r_i)$ into consideration,

$$\begin{aligned} &-\xi_1^t(r_f - r_i) \\ &= -\xi_1^t R\{\nabla G(r_f) - \nabla G(r_i)\} \\ &= -\xi_1^t R\{\nabla G(r_f) + \xi_2\} \\ &= -R\|\nabla G(r_f)\| \|\xi_1\|\cos\left(\varphi + \frac{\pi}{2}\right) \\ &= R\sin\varphi \end{aligned} \tag{13}$$

By replacing $\xi_1^t(r_f - r_i)$ and $-\xi_2^t(r_f - r_i)$ with R(1–cosφ) and Rsinφ, respectively, we finally obtain

$$S_x - S = R\sin\varphi \tag{14}$$

$$\frac{fS^3}{3EI} = S\theta_{add} - R(1\text{–}\cos\varphi) \tag{15}$$

From eqs. (4), (5), (6), (14), and (15), we can derive the following form by applying the first order linear approximation.

$$3EIC_{\theta c} = k(h)S_x, \tag{16}$$

where

$$k(h) = 1 - \frac{1}{2h}, \tag{17}$$

$$h = \frac{S_x}{R\theta_{add}}. \tag{18}$$

Defining the rotational compliance for an edged environment with C_θ, we have the following relationship for such an environment [1], [2],

$$3EIC_\theta = S_x \tag{19}$$

By dividing each side of eq.(16) by that of eq.(19), we can obtain,

$$\frac{C_{\theta c}}{C_\theta} = k(h) \tag{20}$$

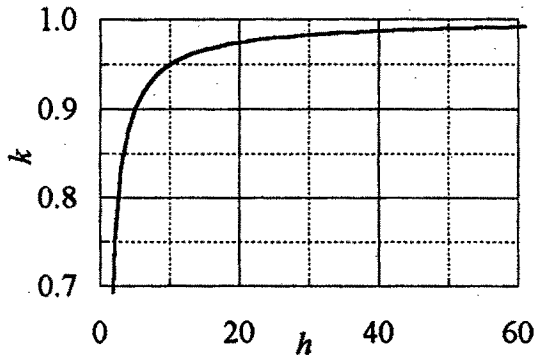

Fig.3 The relationship between k and h

Therefore, k(h) denotes the ratio of the rotational compliance for a circular and an edged environments. For example, k(h)=0.99 means that the theoretical sensing error between a circular and an edged environments is 1%. k(h) is the function of h alone. Since h is composed of the contact distance, the radius of the curvature of the environment, and the pushing angle, the sensing error is also affected by these physical parameters. But an important feature is that the

influence on the sensing error is same as far as the non-dimensional parameter h is identical. Fig.3 shows the map of k(h) for various h. As h increases, k sharply increases and asymptotically saturates to unity for an infinite h. Since an edged environment with a negligibly small R at the point of contact is equivalent to an infinite h, the saturation to unity for an infinite h in Fig.3 is quite reasonable and matches with our intuition. The non-dimensional parameter h given by eq.(18) further suggests that either a contact with extremely long distance from the base or a negligibly small pushing angle also produces a similar effect on the sensing accuracy.

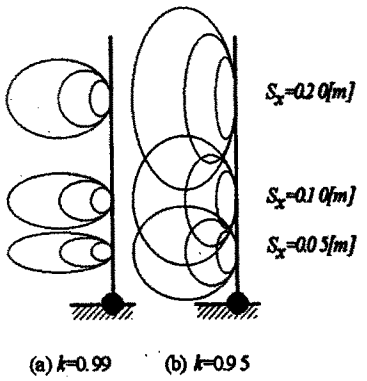

Fig.4 Objects' shape whose errors are 1% and 5%.

Fig.4 visually illustrates objects' shape whose sensing error lead to either 1% or 5%, where the pushing angle is fixed to $\theta_{add}=\pi/36$[rad]. Since a calibration test is normally done for an edged environment, it is desirable that the rotational compliance is insensitive to the curvature of the environment at the point of contact. It can be seen from Fig.4 that the influence of the environment's curvature on the sensing error is suppressed within a few percentages, unless the radius of curvature is extremely large and the contact happens just close to the base.

V. Experiments

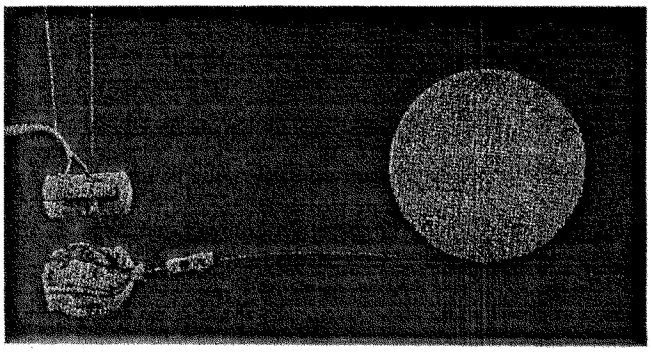

Fig.5 An overview of experimental system

We have developed a hardware model capable of achieving Active Antenna, where a flexible antenna is fixed to an adapter connected to the shaft of actuator. Fig.5 shows an overview of the experimental system. Fig.6 shows the geometrical parameters of the sensor system developed. Strain gauges are glued to a part of the connector to utilize as a torque sensor as shown in Fig.6. Although the discussions taken in section IV assume that the beam is directly connected to the center of the joint axis, an actual experimental system requires an adaptor whose length is (L_1+L_2) to connect the beam to the shaft. The existence of adaptor makes a difference between the model used in section IV and the experimental model. By considering the geometry of the adaptor, we can rewrite the rotational compliance as follows:

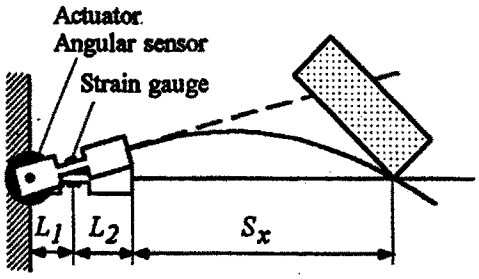

Fig.6 Sensor geometry of the experimental system

$$3EIC_{\theta}=\frac{S_x^3}{(S_x+L_2)(S_x+L_1+L_2)} \tag{21}$$

$$3EIC_{\theta c}=\frac{(S_x-R\varphi)^3}{(S_x-R\varphi+L_2)(S_x-R\varphi+L_1+L_2)} \tag{22}$$

$$\text{where } \varphi=\frac{2h+1-\sqrt{(2h-1)^2-\frac{24}{R\theta_{add}}(L_1+L_2)}}{4}\theta_{add}$$

Fig.7 shows experimental results for a circular object with its radius of R=12mm, where these experiments are done for three different pushing angles $\theta_{add}=\pi/60$, $\pi/36$, and $7\pi/180$, respectively. The real curved lines are theoretical lines obtained by eq.(21) and (22). The small bars and the black pasted squares denote the standard deviations mean values for ten times data obtained for each contact point. As the pushing angle increases, the standard deviations become small. This is because a larger torque caused by a large pushing angle relatively suppresses the noise level with respect to the true signal level. We can see from Fig.7 that the agreement between theoretical and experimental results are fairly good for all pushing angles. It also can be seen that for such an object, the sensing errors due to the object's curvature are less than 1% over the whole contact points and negligibly small.

VI. Conclusions

We have discussed the influence of the environment's curvature on the sensing accuracy. We have shown that the sensing accuracy is controlled only by the non-dimensional parameter h composed of the contact distance, the radius of the curvature of the environment, and the pushing angle. Through the theoretical and experimental analysis, the environment's curvature little influences on the sensing accuracy, and can neglect the effect except for either the contact happens very close to the base or the environment's curvature is extremely small. Finally, the authors would like to express their sincere gratitude to Mr. Y. Hino for his help with experiments.

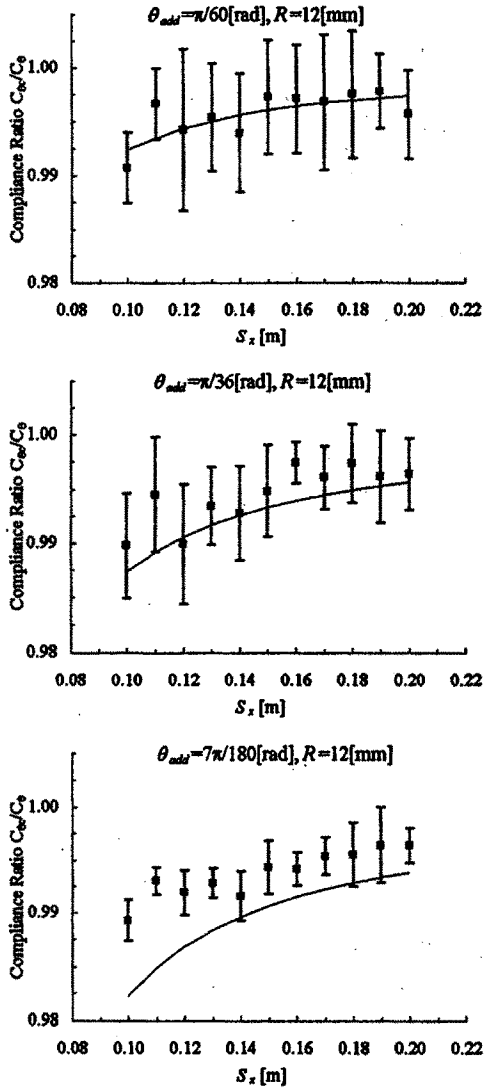

Fig.7 Experimental results of compliance ratio between an edged and a curved objects.

References:

[1]Kaneko, M: Active Antenna, *Proc. of the 1994 IEEE Int. Conf. on Robotics and Automation*, pp2665-2671, 1994.

[2]Kaneko, M., N. Ueno, and T. Tsuji, Active Antenna (Basic Working Principle) *Proc. of the 1994 IEEE Int. Conf. on intelligent Robotics and Systems*, pp1744-1750, 1994.

[3]Kaneko, M., N. Kanayama, and T. Tsuji, 3D Active Antenna for Contact Sensing, *1995 IEEE Int. Conf. on Robotics and Automation at Nagoya*, 1995 (To appear).

[4]Kaneko, M., H. Maekawa, and K. Tanie, Active Tactile Sensing by Robotic Fingers Based on Minimum-External-Sensor-Realization, *Proc. of the 1992 IEEE Int. Conf. on Robotics and Automation*, pp1289-1294, 1992.

[5]Russell, R. A.: Closing the sensor-computer-robot control loop, *Robotics Age*, April, pp15-20, 1984.

[6]Wang, S. S. M., and P. M. Will: Sensors for computer controlled mechanical assembly, *The Industrial Robot*, March, pp9-18, 1978.

[7]McKerrow, P.: Introduction to Robotics, *Addison-Wesley*, 1990.

[8]Brooks, R. A.: A robot that walks; Emergent behaviors from a carefully evolved network, *Neural Computation*, vol.1, pp253-262, 1989.

[9]Hirose, S., et. al.: Titan III: A quadruped walking vehicle, *Proc. of the Second Int. Symp. on Robotics Research*, MIT Press, Cambridge, Massachusetts, 1985.

[10]Schiebel, E. N., H. R. Busby, K. J. Waldron: Design of a mechanical proximity sensor, Robotica, vol.4, pp221-227, 1986.

[11]Russell, R. A.: Using tactile whiskers to measure surface contours, *Proc. of the 1992 IEEE Int. Conf. on Robotics and Automation*, pp1295-1300, 1992.

[12]Tsujimura, T. and T. Yabuta: A tactile sensing method employing force/torque information through insensitive probes, *Proc. of the 1992 IEEE Int. Conf. on Robotics and Automation*, pp1315-1320, 1992.

[13]Salisbury, J. K.: Interpretation of contact geometries from force measurements, *Proc. of the 1st Int. Symp. on Robotics Research*, 1983.

[14]Brock, D.L. and S.Chiu, Environment perception of an articulated robot hand using contact sensors, *Proc. of IEEE Int. Conf. on Robotics and Automation*, Raleigh, 89-96, 1987.

[15]Tsujimura, T. and T. Yabuta, Object detection by tactile sensing method employing force/moment information, *IEEE Trans. on Robotics and Automation*, vol.5, no.4, 1988.

[16]Bicchi, A., Intrinsic contact sensing for soft fingers, *Proc. of IEEE Int. Conf. on Robotics and Automation*, Cincinnati, OH, p968, 1990.